The effect of glucose on the mobility of membrane-adhering liposomes

Jurriaan J. J. Gillissen[†,‡,⊥], Seyed R. Tabaei[†,‡,⊥], Joshua A. Jackman[†,‡], and Nam-Joon Cho[*,†,‡,§]

[†]School of Materials Science and Engineering, Nanyang Technological University, 50 Nanyang Avenue 639798, Singapore
[‡]Centre for Biomimetic Sensor Science, Nanyang Technological University, 50 Nanyang Drive 637553, Singapore
[§]School of Chemical and Biomedical Engineering, Nanyang Technological University, 62 Nanyang Drive 637459, Singapore

*E-mail: njcho@ntu.edu.sg

[⊥]These authors contributed equally to this work.

Abstract

Enclosed lipid bilayer structures, referred to as liposomes or lipid vesicles, have a wide range of biological functions, such as cellular signaling and membrane trafficking. The efficiency of cellular uptake of liposomes, a key step in many of these functions, is strongly dependent on the contact area between a liposome and a cell membrane, which is governed by the adhesion force, the membrane bending energy and the osmotic pressure. Herein, we investigate the relationship between these forces and the physicochemical properties of the solvent, namely the presence of glucose (a nonionic osmolyte). Using fluorescence microscopy, we measure the diffusivity D of small (~50 nm radius), fluorescently labeled liposomes adhering to a supported lipid bilayer or to the freestanding membrane of a giant (~10 μm radius) liposome. It is observed that glucose in solution reduces D on the supported membrane, while having negligible effect on D on the freestanding membrane. Using well-known hydrodynamic theory for the diffusivity of membrane inclusions, these observations suggest that glucose enhances the contact area between the small liposomes and the underlying membrane, while un-affecting the viscosity of the underlying membrane. In addition, quartz crystal microbalance experiments showed no significant change in the hydrodynamic height of the adsorbed liposomes, upon adding glucose. This observation suggests, that instead of osmotic deflation, glucose enhances the contact area via adhesion forces, presumably due to the depletion of the glucose molecules from the intermembrane hydration layer.

Introduction

Spherical lipid bilayers, referred to as lipid vesicles or liposomes, when man-made, [1] have received a great deal of attention due to their relevance in biology, where they occur as transport secretory vesicles[2-3] and cell-derived extracellular vesicles[4] among other classes of biological nanoparticles. In many studies, liposomes are produced artificially and are used as model systems to mimic cell membrane-related processes. [1 5-7] Artificial liposomes are also being used as nanoscale carriers in drug delivery applications.[8-10] Cellular uptake of natural vesicles or artificial liposomes involves membrane bending and fusion.[11-12] Consequently, the uptake rate depends on the contact area between the liposomes and the host membrane.[13-15] The contact area is associated with the liposome shape, which is governed by the adhesion force, the membrane bending energy and the osmotic pressure.[16-24] While adhesion and uptake of natural vesicles is mediated by receptor ligand interactions, the present work focuses on adhesion of artificial liposomes on artificial membranes, without the intervention of membrane proteins. Our work is therefore relevant for applications with artificial liposomes, such as the above-mentioned drug delivery systems.

In this work, we electrostatically adhere negatively charged liposomes onto a positively charged membrane surface, and we study the liposome-membrane interaction, by monitoring the Brownian motion of the membrane-adhering liposomes. In previous work, we observed, that in this system, the liposome diffusivity D is equivalent to that of a cylindrical membrane inclusion. This observation suggests, that the Brownian motion of the liposome is electrostatically slaved to that of a disk-shaped lipid cluster in the underlying membrane. [25 26 27] The size of the cluster is referred to as the contact area. Similar behavior has also been observed for D of covalently bound or molecularly tethered, membrane-adhering colloids or liposomes. [28 29 30] These observations support, that the Brownian motion of membrane-adhering colloids or liposomes is coupled to that of lipid clusters that move in the underlying membrane. When adopting this view, measuring D provides insight into the forces that determine the contact area between the liposome and the underlying

membrane, being the adhesion force, the bending energy and the osmotic pressure, as schematically illustrated in Fig. 1a.

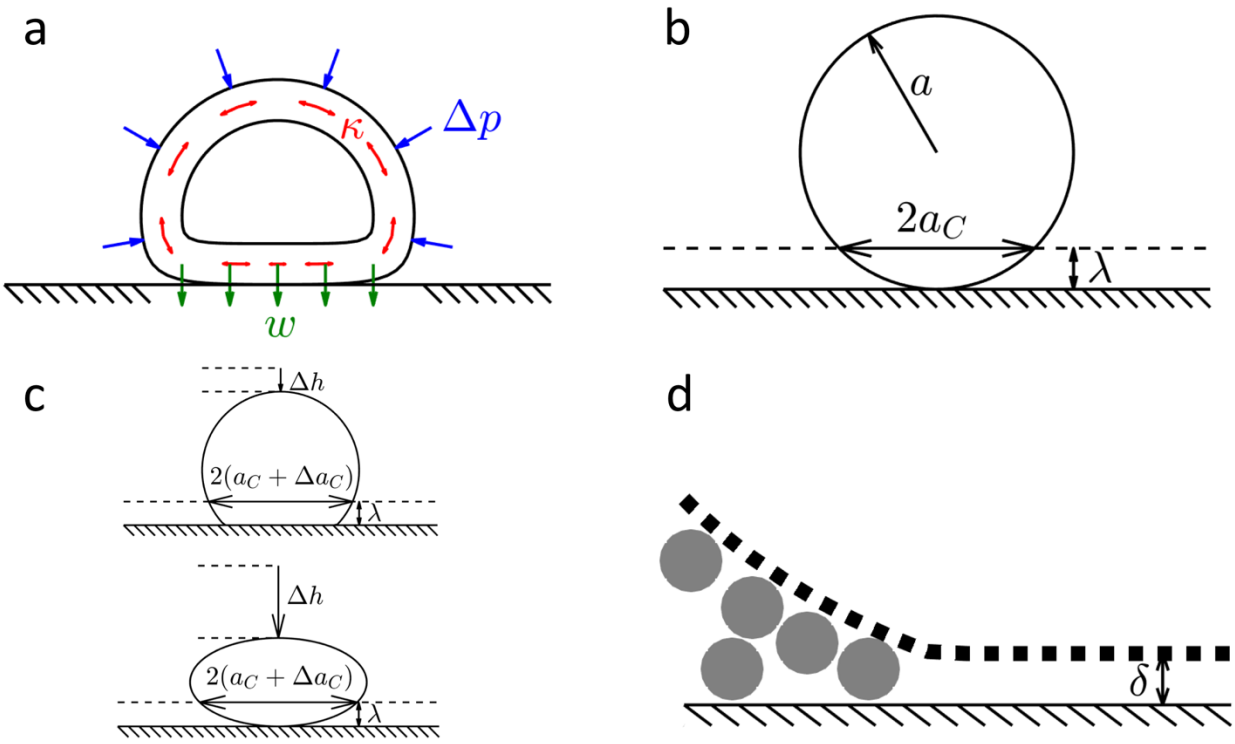

Figure 1. (a) Schematic representation of a surface-adhering liposome, that may be deformed by the osmotic pressure Δp and the surface adhesion force w. Deformation is counteracted by the membrane bending energy κ. **(b)** The inclusion radius a_C is modeled as the circular region in the supported bilayer, which is within one Debye length λ of the liposome. **(c)** Adhesion forces deform the liposome locally at the liposome-substrate contact line, without appreciably changing the liposome height (lower), while osmotic deflation is accompanied by significant changes in the liposome height (upper). **(d)** It is hypothesized that glucose molecules (grey circles, ~1.5 nm) are depleted from the intermembrane hydration layer ($\delta \sim 1$ nm), resulting in adhesion forces. The liposome membrane is indicated with the dotted line.

Following this approach, we have previously studied the diffusivity of small (~50 nm radius) electrically charged liposomes that are adhering to an oppositely charged supported lipid bilayer, suspended in a salt solution.[26-27] It was found that reducing the concentration of the salt (ionic osmolyte) reduces the diffusivity, which reflects an enhanced contact area (or contact radius a_C) due to a reduced screening (*i.e.* an increase) of the electrostatic adhesion force.[26]

The diffusivity data agreed well with the diffusivity model for membrane inclusions, [31]

where the inclusion (contact radius a_C) was modeled as the circular region in the supported bilayer, which is within one Debye length λ of the liposome; see Fig. 1b and see supporting section S9 for a derivation:

$$a_C = \sqrt{2a\lambda}. \quad (1)$$

Eq. (1) is applicable, when $a >> \lambda$, which is not satisfied for nanometer-sized objects, such as proteins, [32] where the contact area is of the order of a few lipids.

In previous work, we furthermore found that diffusivity is insensitive to the charge density in the opposing membranes. [12, 26 27] These observations support, that the contact area between the liposome and the membrane depends on solvent properties via the Debye length, rather than on the surface adhesion force, which depends on the membrane charge densities. It is further noted, that charge exchanges between the liposome and the membrane on a time scale ~10^3 s, and has no significant effect on the liposome diffusivity. [12, 33]

In previous work, we furthermore found that adding glucose (nonionic osmolyte) reduces the diffusivity, and we elucidated the governing mechanism, by applying a shear flow over the membrane.[27] By measuring both the diffusivity as well as the shear-induced drift velocity of the liposomes, we computed the hydrodynamic height of the liposomes, showing negligible change after adding glucose. Assuming that the membrane viscosity is unaltered, this observation would suggest, that glucose extends the intermembrane contact area via adhesion forces, rather than via osmotic forces. This conclusion is supported by deformation calculations in supporting section S10. There, it is shown, that osmotic deflation would appreciably change the liposome height, while adhesion forces would enhance the contact area without appreciably changing the liposome height. This is related to the nature of this type of deformation, which is localized at the liposome-substrate contact line, as illustrated in Fig. 1c. In Ref. [27] it was hypothesized, that the responsible adhesion force is a "depletion force". Owing to its large size (~1.5 nm), it is conceivable that glucose molecules are depleted from the intermembrane hydration layer (~1 nm),[34] causing an adhesive

107 force,[35-36] as illustrated in Fig. 1d.

108 Furthermore, the absence of glucose-induced osmotic deflation suggests that the liposomes
109 were already maximally deformed in the absence of glucose, presumably due to the liposome-
110 membrane adhesion force. The absence of osmotic deflation might suggest, that pores form in the
111 membrane, equilibrating the transmembrane osmotic pressure. However, the time scale for the
112 trans-membrane transport due to pore formation is likely larger than the experimental time scale;
113 see e.g. Ref. [37]. Alternatively, we have previously argued, that osmotic deflation could be
114 counteracted by a relatively large membrane bending energy κ, which is expected to increases as
115 the radius of curvature of the liposome diminishes and approaches the membrane thickness,
116 inhibiting liposome deformation beyond a certain threshold; see, *e.g.*, Refs. [38, 39].

117 In the present work, we further study the effect of glucose on the diffusivty D of membrane-
118 adhering liposomes, scrutinizing the roles of the adhesion force, the contact area and the associated
119 liposome deformation. First, we confirm that glucose reduces D due to an enhanced contact area a_C,
120 and not due to a modulation of the membrane viscosity η_M. To this end, we compare the glucose-
121 induced change in D of liposomes adhering to a supported and a free-standing membrane.
122 According to well-established hydrodynamics theory, the former is rather insensitive to η_M and
123 sensitive to a_C [31] [see Eq. (5) below], while the latter is insensitive to a_C, and sensitive to η_M [40] [see
124 Eq. (6) below]. The observation of a reduced D on the supported membrane, and an unaffected D on
125 the giant liposome, confirms that glucose enhances a_C, while leaving η_M intact. Secondly, we
126 elucidate the origin of the enhanced a_C, by measuring the associated glucose-induced change in
127 liposome height, using the quartz crystal microbalance technique. [39] The observation of a negligible
128 height change, suggests that instead of the osmotic pressure, it is the adhesion force that enhances
129 a_C. These results confirm our previous findings, that glucose inhibits the diffusivity of supported
130 bilayer-adhering liposomes via adhesion forces. [27] There it was hypothesized that this adhesion
131 force originates from a depletion of the glucose molecules from the intermembrane hydration

layer.[27]

Results

Liposome Diffusivity on Supported Membranes

Positively charged supported lipid bilayers are produced using the liposome fusion method[41] on the glass wall of a fluidic chamber. Then fluorescently labeled and negatively charged, small unilamellar liposomes, which serve as tracking particles, are injected into the fluidic chamber, where they adhere to and diffuse on the positively charged supported bilayer. The mean radius of the liposomes a = 51 nm was measured using dynamic light scattering (DLS); see supporting Fig. S1.

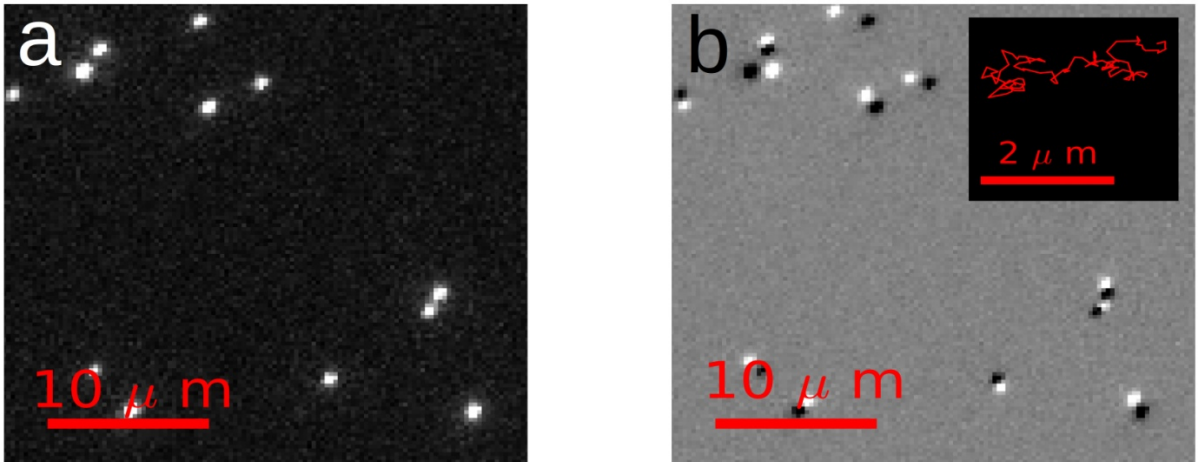

Figure 2 Fluorescence microscopy is used to measure the diffusivity of small liposomes on supported lipid bilayers. (a) A 50 × 50 μm section of a 137 × 137 μm fluorescence microscopy image. The liposomes appear as bright spots. (**b**) Visualization of liposome motion by subtracting two TIRF images that are separated by four seconds, *i.e.* by 80 frames. The displaced liposomes appear as pairs of bright and dark spots. The inset shows a liposome trajectory, that is reconstructed by matching the liposome positions in subsequent images.

A section of a fluorescence image is given in Fig. 2a, showing the supported membrane, with membrane-adhering liposomes (bright spots). Fig. 2b visualizes the liposome motion, by subtracting two images with a four seconds time interval (80 frames), which corresponds to a liposome displacement of roughly 2 μm or 8 pixels. The displaced liposomes appear as pairs of bright and dark spots. Particle tracking is used to reconstruct the trajectories of the liposomes from

the fluorescence images (see supporting section S7). A typical trajectory is shown in the inset of Fig. 2b.

Fig. 3a shows the liposome displacement probability density function $G(r, t)$ on a logarithmic y-axis as a function of the scaled, squared displacement $r^2/4t$ for various fixed values of the elapsed time t. The function is constructed from all measured position pairs on all detected trajectories. On these coordinates, the data for different times collapse on a straight line, which implies that the displacements are Brownian and Gaussian:

$$G(r,t) = \exp\left[-r^2(4Dt)^{1/2}\right](4\pi Dt)^{-1/2}. \quad (2)$$

Here, D is the overall (ensemble averaged) diffusivity. To further confirm the Brownian character of the liposome diffusivity, the inset of Fig. 3a shows, that the ensemble-averaged (over all liposomes) mean squared displacement (MSD) is a linear function of the elapsed time t. Next, the MSD was computed for individual liposomes and the resulting diffusivity distribution is presented in Fig. 3b, showing a mean and standard deviation of $D = 0.30 \pm 0.33$ μm^{2}s^{-1}. This value for D is reasonably close to the observed diffusivity $D = 0.2$ μm^{2}s^{-1} for liposomes, that were tethered with DNA segments to individual lipids in the underlying supported membrane.[29] This similarity supports the hypothesis in Ref. [29], that the tethered liposomes experiences direct contact with the underlying membrane, suggesting a similar frictional origin to the observed diffusivity as in the present study.

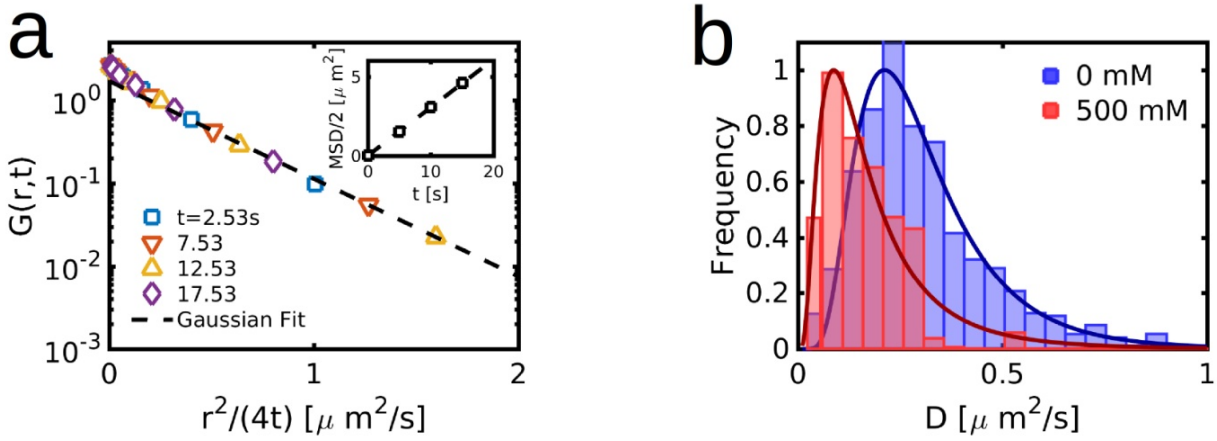

Figure 3 Displacement and diffusion statistics of small liposomes adhered on supported lipid bilayers. (a) Probability density $G(r, t)$ as a function of the scaled, squared liposome displacement $r^2/4t$ on a logarithmic y-axis. The collapse of the data for different times on a straight line reveals that the diffusion is Brownian and Gaussian [Eq. (2)]. The inset shows the ensemble averaged (over all liposomes) mean squared displacement (MSD) as a function of the

elapsed time. The straight line confirms that the motion is Brownian. (**b**) Diffusivity D histogram, before and after adding 500 mM glucose to the liposome environment. The observed reduced diffusivity reflects an enhanced contact area between the liposome and the supported bilayer.

It is re-emphasized, that we interpret the liposome diffusivity data, by assuming, that the Brownian motion of the liposome is electrostatically slaved to that of a disk-shaped cluster of lipids in the underlying membrane.[25-27] The size of the cluster is referred to as the contact area, which is defined as the membrane region, within one Debye length to the liposome; see Fig. 1b. The corresponding model for the contact radius [Eq. (1)] has been experimentally verified, by measuring D at various salt concentrations. [26] In this framework, the liposome diffusivity D is equivalent to that of the disk-shaped lipid cluster, that moves within the underlying membrane, which is given by the Evans-Sackmann model for the diffusivity of inclusions in supported fluidic membranes:[31]

$$D = \frac{k_B T}{4\pi\eta_M} \frac{1}{\left(\frac{1}{2}\varepsilon^2 + \frac{\varepsilon K_1(\varepsilon)}{K_0(\varepsilon)}\right)}, \text{ where } \varepsilon = a_C\sqrt{\frac{b}{\eta_M}}. \quad (3)$$

Here, k_BT is the Boltzmann energy, a_C is the inclusion radius, η_M is the membrane viscosity, K_0 and K_1 are the zeroth and first order modified Bessel functions of the second kind, and b is a phenomenological friction coefficient, to account for the presence of the solid support. Since the disk is an intrinsic part of the membrane, it experiences the same friction with the underlying support as the rest of the membrane, i.e. $b_p = b_s$ in Eq. (3.3) in Ref. [31]. If the disk would experience no friction with the support, then $b_p = 0$ in Eq. (3.3) in Ref. [31], and the factor ½ inside the bracket of Eq. (3) would be ¼. Parameter $\varepsilon = a_C/a^*$ is the dimensionless inclusion radius, where $a^* = (\eta_M/b)^{½}$ is a characteristic length scale, that defines a crossover between two regimes. In the first regime, the radius is relatively small $a_C << a^*$ ($\varepsilon << 1$), such that the second term within the brackets on the r.h.s. of Eq. (3) dominates, and the diffusion is predominantly governed by the membrane viscosity, and reads:

$$D = \frac{k_B T}{4\pi\eta_M} \frac{1}{\log\left(\sqrt{\frac{\eta_M}{b a_C^2}}\right)}, \quad \text{when:} \quad a_C \ll \sqrt{\frac{\eta_M}{b}}. \quad (4)$$

In the second regime, the inclusion radius is relatively large: $a_C >> a^*$ ($\varepsilon >> 1$), such that the first

term within the brackets on the r.h.s. of Eq. (3) dominates and the diffusion is predominantly governed by the friction with the solid support, and reads:

$$D = \frac{k_B T}{2\pi a_C^2 b}, \quad \text{when:} \quad a_C \gg \sqrt{\frac{\eta_M}{b}}. \tag{5}$$

Since we are concerned with the diffusivity of a lipid cluster in the upper leaflet of the supported bilayer, we interpret b and η_M in Eq. (3) as the inter-leaflet friction coefficient and the monolayer viscosity, respectively, which is half the bilayer viscosity. [26, 42] In our system, the ionic strength is 150 mM (NaCl) and the (mean) liposome radius is a = 51 nm, which gives for the Debye length: λ = 0.8 nm and for the contact radius: a_C = 9 nm. Using these values together with $b = 2 \times 10^7$ kg s^{-1}m^{-2} and η_M = ½ 4 × 10^{-10} kg s^{-1}(mono-layer viscosity),[42] we find D = 0.22 μm^{2}s^{-1}, which is reasonably close to the measured value of D = 0.30 μm^{2}s^{-1}. This agreement validates a_C = 9 nm [Eq. (1)] as a reasonable estimate for the contact radius between the membrane-adhering liposomes and the supported bilayer. With these parameter values, we estimate: ε = 2.8, which means that the diffusivity has a strong size dependence, and is rather insensitive to the membrane viscosity η_M, as given by the limiting relation Eq. (5).

It is noted, that in a previous work, we have independently measured $b = 1 \times 10^7$ kg s^{-1}m^{-2},[26] close to the value, used above. [42] In addition, we have previously measured the membrane (mono-layer) viscosity, using a particle tracking technique on GUVs, [25] and on SLBs, [26] both giving η_M = 2 × 10^{-10} kg s^{-1}, consistent with the value used above, [42] and with independent measurements in the literature; see e.g. Refs [43 44 30]. It is noted, that in the literature, there is a large variation of measured values for η_M, and a strong dependence on membrane constitution. For instance, gel-phase or cholesterol-rich membranes show large η_M, [45] which is several orders of magnitude larger than for the single-phase, and fluid-phase membranes, used here.

In Fig. 3b we study the effect of glucose by comparing the distribution of liposome diffusivity on the supported bilayer before and after adding 500 mM glucose to the solution. We measure that the glucose induces a 50% reduction in the liposome diffusivity from D = 0.30 ± 0.33

$\mu m^2 s^{-1}$ to $D = 0.15 \pm 0.27$ $\mu m^2 s^{-1}$. According to Eq. (5), the diffusivity is insensitive to the membrane viscosity η_M and strongly depends on the contact area a_C. Therefore, these measurements suggest, that the glucose reduces D by an increase in a_C, while changes in η_M play an insignificant role.

Liposome Diffusivity on Freestanding Membranes

We further scrutinize the effect of the contact area and the membrane viscosity on the diffusivity of membrane-adhering liposomes. To this end we measure the diffusivity of liposomes adhering to a free-standing membrane, which, as opposed to the supported bilayer [Eq. (5)], is rather insensitive to the contact area, but sensitive to the membrane viscosity [see Eq. (6) below]. Again, we consider the effect of glucose, and any observed change in the diffusivity would support, that glucose alters the membrane viscosity.

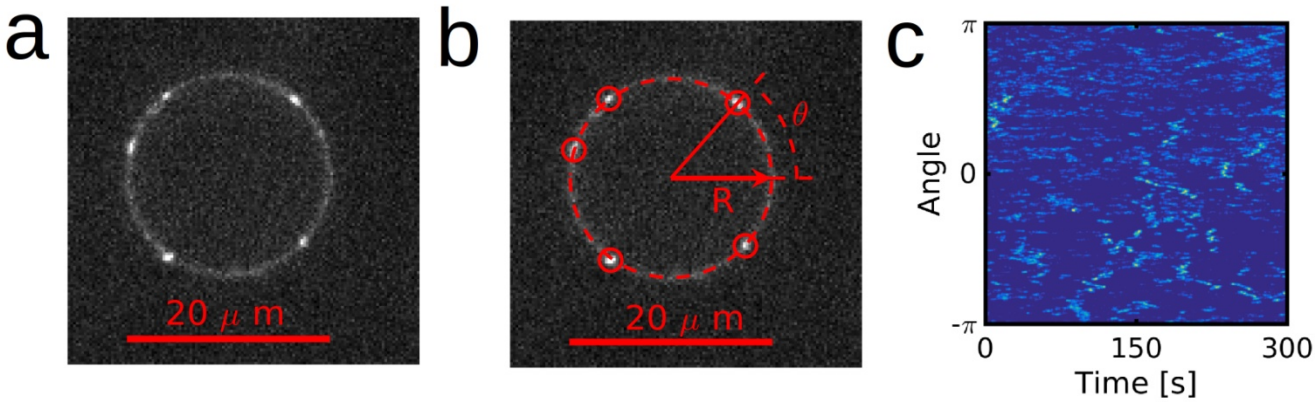

Figure 4. Confocal microscopy is used to measure the diffusivity of small liposomes adhering to giant liposomes. **(a)** Confocal microscopy image of a giant liposome that is decorated with small liposomes. The small liposomes appear as bright spots. **(b)** Detected giant liposome rim (dashed line) and small liposomes (encircled). The position of the small liposome is expressed in polar coordinates: R and θ. (**c**) Detected liposome angles θ at various time instances t are visualized as bright spots on the (θ, t) plane.

Negatively charged, fluorescently labeled, small liposomes are electrostatically targeted onto positively charged, giant (~10 μm radius), unilamellar liposomes. [25] The mean radius of the small liposome a = 56 nm is measured using nano-particle tracking analysis (NTA); see supporting Fig. S1. The giant liposomes are fabricated using the electroformation method.[46] Confocal microscopy is used to measure the polar angle θ of the liposome positions on the equatorial rim with radius R of

the giant liposome (Figs. 4a,b). In the confocal microscopy images, the liposomes appear to execute one-dimensional motion along the equatorial rim (Fig. 4c). There was no visible sign of thermal, so-called Helfrich fluctuations,[47] in the membrane of the giant liposome. These fluctuations are therefore ignored in the analysis, and we assume that the small liposomes diffuse on a static membrane surface.

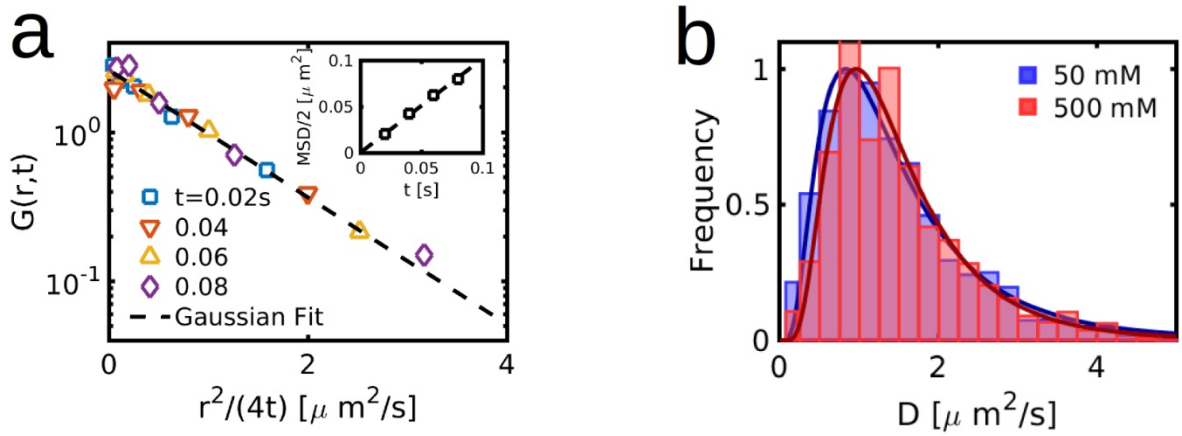

Figure 5. Displacement and diffusivity statistics of small liposomes adhering to giant liposomes (a) Probability distribution $G(r, t)$ as a function of the scaled, squared liposome displacement $r^2/4t$ on a logarithmic y-axis. The data for different times collapse on a straight line, which indicates that the motion is Brownian and that the displacement statistics are Gaussian [Eq. (2)] The inset shows the ensemble averaged (over all liposomes) mean squared displacement (MSD) as a function of the elapsed time. The straight line confirms that the motion is Brownian. (**b**) Diffusivity D histograms before and after adding 500 mM glucose to the liposome environment show no noticeable difference.

The probability density function $G(r, t)$ of the liposome displacement along the rim coordinate $r = R\theta$ collapses on a straight line on ($r^2/4t$, log G) – coordinates (Fig. 5a), which implies Brownian and Gaussian displacement statistics. Brownian motion is further confirmed by the linear dependence of the ensemble averaged MSD on time, shown in the inset of Fig. 5a. Liposome diffusivities are computed from the slope of the MSD curves for the individual liposomes. The resulting distribution (Fig. 5b) shows that liposome diffusivity $D = 1.46 \pm 0.96$ μm^{2}s^{-1} is five-fold larger on the giant liposome than on the supported bilayer $D = 0.30 \pm 0.33$ μm^{2}s^{-1} (*cf.* Fig. 3b). The diffusivity of individual lipids is roughly twice as large in free-standing membranes as in solid supported membranes. [48] The lower diffusivity for supported membranes of either liposomes or individual lipids, both originate from friction with the support. For the case of liposomes however, this friction is more pronounced, *i.e.*, a five-fold reduction in D versus a two-fold reduction for

individual lipids. [48] Since according to Eq. (5), the friction with the support scales with the area, these observations support, that the Brownian motion of the liposome is coupled to that of an area of lipids in the underlying membrane.

On the free-standing membrane, on the other hand, there is no such area dependence, and the diffusivity of inclusions in the free-standing membrane is governed mainly by the membrane viscosity η_M, according to the Saffman – Delbrück model: [40]

$$D = \frac{k_B T}{4\pi\eta_M}\left(\log\left[\frac{\eta_M}{\eta a_C}\right] - \gamma\right). \quad (6)$$

Here $\gamma \approx 0.58$ is Euler's constant, η is the viscosity of the 3D medium and η_M is the viscosity of the 2D membrane. Eq. (6) accounts for viscous friction with the surrounding liquid, under the assumption that $\eta/(h\eta_M) << 1$, where h is the membrane thickness. It is further noted, that Eq. (6) assumes a no-slip condition between the disk and the surounding membrane. A free-slip condition would add a term of +1/2 to the round brackets in Eq. (6).[49] As we are dealing with a cluster of lipids, the exact boundary condition is uncertain. However, the +1/2 - term is of minor importance for the qualitative dependence of D on cluster size a_C and on membrane viscosity η_M.

In contrast to the diffusivity of inclusions in supported membrenes [Eq. (5)], which depends on a_C and is sensitive towards η_M, the diffusivity of inclusions in free-standing membranes [Eq. (6)] has opposite behavior, with a strong dependence on η_M, while rather insensitive (logarithmic dependence) to a_C. This weak a_C dependence is a signature of the quasi two-dimensional nature of the hydrodynamic system.[40]

Eq. (6) predicts $D = 2.6$ μm^{2}s^{-1}, which is reasonably close to the measured $D = 1.46 \pm 0.96$ μm^{2}s^{-1} based on $\eta_M = 4 \times 10^{-10}$ kg s^{-1} (bilayer viscosity),[42] and modeling the inclusion radius a_C with Eq. (1), using a liposome radius of $a = 56$ nm and a Debye length of $\lambda = 0.8$ nm. However, the exact value of a_C is, of minor importance as it appears inside the logarithm of Eq. (6).

Fig. 5b shows that adding 500 mM glucose does not significantly affect the liposome diffusivity on the giant liposome membrane, *i.e.* it changes from $D = 1.46 \pm 0.96$ μm^{2}s^{-1} to $D = 1.56$

300 ± 1.04 $\mu m^2 s^{-1}$. This is in contrast to the situation on the supported membrane, where a 50%
301 reduction in liposome diffusivity was observed upon adding 500 mM glucose (*c.f.* Fig. 3b). The
302 insensitivity of the liposome diffusivity on the giant liposome membrane suggests that glucose does
303 not alter the membrane viscosity. This result supports, that the observed, reduced diffusivity on the
304 supported bilayer is due to an increase in the contact area between the liposome and the supported
305 bilayer.

306 Liposome Deformation on the Quartz Crystal Microbalance

307 Finally, we address the question, whether glucose enhances the contact area through osmotic forces
308 or due to adhesion forces. To address this issue, we consider the associated deformation of the
309 liposome. In supporting section S10, we demonstrate, that osmotic forces would significantly
310 reduce the liposome height, while adhesion forces would deform only at the liposome-membrane
311 contact line, with negligible changes in the liposome height. This is also illustrated in Fig. 1c.

312 In a previous work, we experimentally addressed this issue, by subjecting membrane-
313 adhering liposomes to a hydrodynamic shear flow. Measuring both the diffusivity and the drift
314 velocity, allowed computing both the contact area and the height of the liposomes. [27] By adding 500
315 mM glucose, the contact area was observed to increase, without appreciable changes in the
316 liposome height. [27] This, together with the analysis in supporting section S10, suggests that glucose
317 induces adhesion forces, which enhance the contact area, without changing the liposome height.

318 It is further noted, that withstanding the osmotic pressure of 500 mM glucose requires a
319 membrane bending energy: $\kappa \sim 10^3\ k_B T$, [39] which is few orders of magnitude larger than what is
320 usually measured for large membrane structures; see *e.g.* Ref. [50]. This suggests, that κ increases,
321 due to steric hindrance of lipid molecules in highly curved membranes. This conclusion has
322 previously been supported by quartz crystal microbalance (QCM-D) measurements, showing a
323 similar, negligible change in liposome height, after adding an ionic osmolyte. [39]

324 Here we use the QCM-D technique to further study the changes in the adsorbed liposome

height, after adding 500 mM glucose. QCM-D measurements are performed on the adsorption of zwitterionic liposomes on solid (TiO_2) supports. Despite using TiO_2 instead of a lipid bilayer, the osmotic pressure is likely the same in both systems. The mean radius of these liposomes, $a = 48$ nm, was measured using DLS, as shown in supporting Fig. S1. Fig. 6a shows the time-dependent (negative) frequency shifts $-\Delta f/n$ for the various overtones n due to liposome adsoprtion in the absence of glucose. During the time interval shown in Fig. 6a, the frequency shifts are linear functions of time, which imply a sufficiently small surface coverage such that the liposomes do not hydrodynamically interact with each other. [39, 51] In this uncoupled regime, liposome deformation can be determined from the overtone-dependence of the frequency shifts,[39] which is shown in Fig. 6b at a fixed time: $t \approx 5$ min.

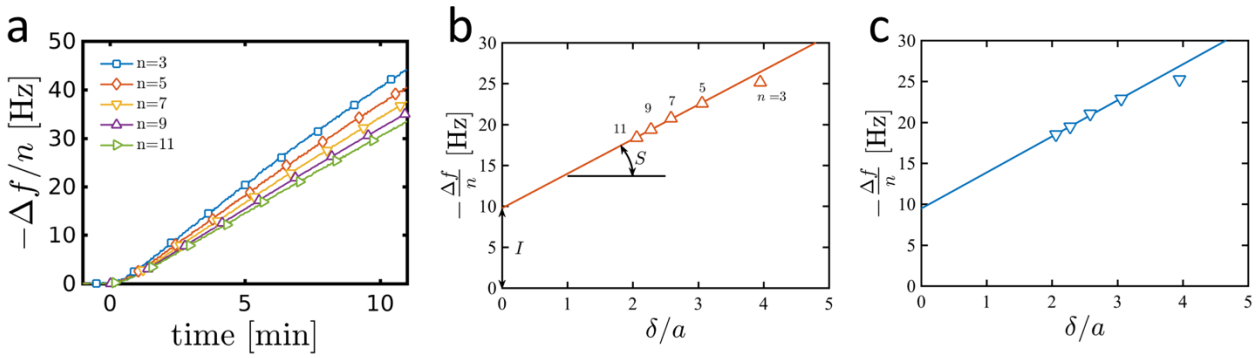

Figure 6. Effect of glucose on liposome deformation, measured by QCM-D. Negative frequency shift $-\Delta f/n$ as a function of time t for various overtones n for liposomes adsorbing on TiO_2 in isotonic buffer solution. (**b**) Frequency shifts (in Hz) for the various overtones at a fixed time: $t \approx 5$ min. The data are plotted on (δ/a, $-\Delta f/n$)-coordinates, where $\delta = (\nu/f_0 n)^{1/2}$ is the (overtone dependent) viscous penetration depth, a is the (un-deformed) liposome radius, f_0 is the QCM-D fundamental frequency and ν is the fluid kinematic viscosity. For $\delta/a < 3$ the data follow a straight line and the liposome aspect ratio $r = 0.74(S/I)^{-0.95}$ is determined from the slope S and the intercept I of this line: $r \approx 1.5$, which corresponds to a modest deformation, presumably induced by the interaction between the liposomes and the TiO_2 substrate. **(c)** Same as in (b) but after adding 500 mM glucose, which gives $r \approx 1.6$, *i.e.*, we do not observe an aprciable liposome height change.

The data are plotted on (δ/a, $-\Delta f/n$)-coordinates, where $\delta = (\nu/f_0 n)^{1/2}$ is the (overtone-dependent) viscous penetration depth, $a = 48$ nm is the (non-deformed) liposome radius, f_0 is the QCM-D fundamental frequency and ν is the fluid kinematic viscosity. On these coordinates, the data follow a straight line for $\delta/a \leq 3$, and following the method in Ref. [51], the liposome aspect ratio $r = 0.74(S/I)^{-0.95}$ is determined from the slope S and the intercept I of this line: $r = 1.5 \pm 0.2$, where the mean and standard deviation are obtained by repeating the experiment three times. This result

corresponds to a modest deformation, presumably induced by the interaction between the liposomes and the TiO_2 substrate. [39] We performed the same experiment for liposomes in 500 mM glucose solution (see Fig. 6c) and found a nearly identical deformation with $r = 1.6 \pm 0.1$. These results suggest that the glucose does not substantially deform the liposomes beyond the deformation, which is induced by the liposome-substrate adhesion force in the absence of glucose.

Conclusion

We have used fluorescence microscopy and particle tracking to measure the diffusivity of liposomes that are electrostatically adhering to supported and free-standing membranes. Adding glucose (a nonionic osmolyte) to the solution is observed to inhibit liposome diffusivity on the supported bilayers, while not affecting the diffusivity on free-standing bilayers. These observations support that glucose enhances the contact area between liposomes and the underlying membrane, while not affecting the viscosity of the membrane.

To elucidate the mechanism for the enhanced contact area, quartz crystal microbalance experiments were conducted, showing that glucose did not induce a significant liposome height change, beyond a modest height change, that was already induced by the substrate (TiO_2) in the absence of glucose. Similar conclusions were previously derived from diffusivity and drift velocity measurements of membrane-adhering liposomes in sheared glucose solutions.[27] Based on geometrical considerations (supporting section S10), the observation of a constant liposome height suggests, that the reduced liposome diffusivity (*cf.* Fig. 3b) is due to adhesion forces, which extend the contact area between the liposome and the membrane, without appreciably changing the liposome height.

As illustrated in Fig. 1d, we speculate that the glucose induces adhesion forces via a depletion effect.[35-36]As the intermembrane hydration layer is on the order of 1 nm, [34] it is conceivable that the glucose molecules (~1.5 nm) are (partly) depleted from this layer, resulting in an adhesion force. While previously observed for macromolecules,[29, 52] this may be evidence of an

adhesion force due to the depletion of small (~ 1 nm) molecules from the intermembrane hydration layer.

In summary, the diffusivity of membrane-adhering liposomes can be manipulated by glucose, *i.e.* a nonionic osmolyte, and we have scrutinized the responsible mechanism by isolating the effects of the contact area, the membrane viscosity and liposome deformation. The present work provides insight into the contact between liposomes and membrane surfaces, where the associated material properties are different at the nano-scale, than at the macroscopic scale. [53] In addition to these material insights, the present work may also offer a practical method to control liposome mobility, which can be used for separation and characterization purposes.

Experimental Section

Liposome Diffusivity on Supported Membranes. A positively charged supported lipid bilayers is produced on the inner glass wall of a fluidic chamber by the liposome fusion method,[41] *i.e.*, by the absorption, rupture and fusion of positively charged, small unilamellar liposomes. For this purpose, we produced positively charged liposomes by extruding a lipid solution with 10 % positively charged 1,2-distearoyl-sn-glycero-3-ethylphosphocholine (chloride salt) (DOEPC) lipids and 90 % zwitterionic phosphatidylcholine (DOPC) lipids with an Avanti Mini- Extruder (Avanti Polar Lipids) using a track-etched polycarbonate membrane with a 100 nm diameter nominal pore size.

Negatively charged and fluorescently labeled liposomes, that serve as tracking particles, were fabricated by extrusion with a composition of 5% negatively charged 1-palmitoyl-2-oleoyl-sn-glycero-3-phospho-L-serine (sodium salt) (DOPS) lipids and 95% DOPC lipids and 1% rhodamine-PE lipids. The size distributions of the corresponding liposomes are measured using nanoparticle tracking analysis (NTA, NanoSight, U.K.) and dynamic light scattering (DLS, Brookhaven Instrument Co., New York, USA) and are given in supporting Fig. S1. The fluorescently labeled and negatively charged liposomes are injected into the fluidic chamber at a flow rate of 40 $\mu L\ min^{-1}$ and a concentration of 4 $mg\ mL^{-1}$ for 1 min, In the chamber the liposomes adhere to the positively

charged supported bilayer, reaching a coverage of roughly one liposome per 100 μm^2 of the supported bilayer, which was sufficiently small to allow the tracking of an individual liposome over sufficient periods of time between two successive encounters with a neighboring liposome. Before measuring the diffusive motions of the liposomes, the chamber is flushed with pure buffer for 1 min, to eliminate that liposomes in the bulk obscure the view to the adhering liposomes. After rinsing fluorescence microscopy images are recorded at 20 fps during a period of 100 s. The image size is 512 × 512 pixels or 136 × 136 μm. Typical liposome displacement between two consecutive frames is 0.25 μm or one pixel. We use particle tracking to reconstruct the trajectories of the liposomes from the fluorescence microscopy images (see supporting sections S5-S7).

Lipid transfer between the liposomes and the supported bilayer results in charge equilibration and consequently liposome detachment.[33] This process however occurs over tens of minutes, which leaves sufficient time to measure the liposome diffusivity. Furthermore, liposome fusion is known to occur above a certain charge density.[54-55] We deliberately eliminate fusion by using charge densities in the liposomes and in the supported bilayers, that are below the fusion threshold, and no signs of fusion were observed.

Liposome Diffusivity on Free-Standing Membranes. Positively charged giant unilamellar liposomes are fabricated at a size of approximately 20 μm using the electroformation method.[46] The composition and the charge of the giant liposome is identical to that of the supported lipid bilayers, *i.e.* 10 % positively charged DOEPC lipids and 90 % zwitterionic DOPC lipids.

Negatively charged liposomes are electrostatically targeted onto the positively charged giant liposome surface at roughly 1 liposome per 100 μm^2. Small liposome positions on the giant liposome surface are measured using confocal microscopy, through the equatorial plane of the giant liposome. Images were recorded at 50 fps during a total time of 300 s. Within the imaged slice, we observe a few liposomes at the same time. Within the confocal image the liposomes appear to describe one dimensional (azimuthal) motion along the equatorial rim. Software was developed to

detect these azimuthal displacements. The residence time of the liposomes within the confocal image was of the order of a few seconds, which corresponds to a few μm azimuthal displacement. This turned out to be sufficient to accurately determine the corresponding diffusion constant.

Liposome Deformation on a Solid Interface. Deformation of zwitterionic (DOPC) liposomes on a titanium oxide substrate was measured using the Quartz Crystal Microbalance-Dissipation (QCM-D) measurement technique. Immediately before injection into the QCM-D flow chamber, the liposomes were diluted to 5 μg mL^{-1} in either buffer or in buffer with additional 500 mM glucose. The relatively small lipid concentration ensured a sufficiently slow adsorption process (≈ 4 Hz min^{-1}) which was required to obtain a reproducible overtone-dependent frequency shift at low coverage. During liposome injection the frequency shifts $\Delta f/n$ were recorded for the 3rd to 11th odd overtones.

Associated Content

Supporting Information

The supporting information provides details on small liposome preparation, small liposome size distribution, giant liposome preparation, supported bilayer formation, confocal fluorescence microscopy, total internal reflection fluorescence microscopy, liposome tracking, QCM-D experiments, contact radius model, liposome deformation due to surface adhesion and due to osmotic pressure. This material is available free of charge via the Internet at Langmuir.

Notes

The authors declare no competing financial interest

Acknowledgements

This work was supported by the National Research Foundation of Singapore through a Competitive Research Programme grant (NRF-CRP10-2012-07) and a Proof-of-Concept grant (NRF2015NRF-POC0001-19) as well as through the Centre for Precision Biology at Nanyang Technological University.

References

1. Bangham, A., Liposomes: the Babraham connection. *Chemistry and physics of lipids* **1993,** *64* (1-3), 275-285.
2. Rizo, J.; Rosenmund, C., Synaptic vesicle fusion. *Nature structural & molecular biology* **2008,** *15* (7), 665-674.
3. Rizzoli, S. O.; Betz, W. J., Synaptic vesicle pools. *Nat Rev Neurosci* **2005,** *6* (1), 57-69.
4. Fuhrmann, G.; Herrmann, I. K.; Stevens, M. M., Cell-derived vesicles for drug therapy and diagnostics: Opportunities and challenges. *Nano Today* **2015,** *10* (3), 397-409.
5. Cornell, B.; Fletcher, G.; Middlehurst, J.; Separovic, F., The lower limit to the size of small sonicated phospholipid vesicles. *Biochimica et Biophysica Acta (BBA) - Biomembranes* **1982,** *690* (1), 15-19.
6. Walde, P.; Cosentino, K.; Engel, H.; Stano, P., Giant vesicles: preparations and applications. *ChemBioChem* **2010,** *11* (7), 848-865.
7. Ostro, M. J., *Liposomes: from biophysics to therapeutics*. Courier Corporation: 1987.
8. Torchilin, V. P., Recent advances with liposomes as pharmaceutical carriers. *Nature reviews: Drug discovery* **2005,** *4* (2), 145-160.
9. Barenholz, Y., Liposome application: problems and prospects. *Current opinion in colloid & interface science* **2001,** *6* (1), 66-77.
10. Chatin, B.; Mevel, M.; Devalliere, J.; Dallet, L.; Haudebourg, T.; Peuziat, P.; Colombani, T.; Berchel, M.; Lambert, O.; Edelman, A.; Pitard, B., Liposome-based Formulation for Intracellular Delivery of Functional Proteins. *Mol Ther Nucleic Acids* **2015,** *4*, e244.
11. McMahon, H. T.; Kozlov, M. M.; Martens, S., Membrane curvature in synaptic vesicle fusion and beyond. *Cell* **2010,** *140* (5), 601-605.
12. Tabaei, S. R.; Gillissen, J. J.; Vafaei, S.; Groves, J. T.; Cho, N.-J., Size-dependent, stochastic nature of lipid exchange between nano-vesicles and model membranes. *Nanoscale* **2016,** *8* (27), 13513-13520.
13. Yang, K.; Ma, Y.-Q., Computer simulation of the translocation of nanoparticles with different shapes across a lipid bilayer. *Nature nanotechnology* **2010,** *5* (8), 579-583.
14. Tree-Udom, T.; Seemork, J.; Shigyou, K.; Hamada, T.; Sangphech, N.; Palaga, T.; Insin, N.; Pan-In, P.; Wanichwecharungruang, S., Shape Effect on Particle-Lipid Bilayer Membrane Association, Cellular Uptake, and Cytotoxicity. *ACS Applied Materials & Interfaces* **2015,** *7* (43), 23993-24000.
15. Gratton, S. E.; Ropp, P. A.; Pohlhaus, P. D.; Luft, J. C.; Madden, V. J.; Napier, M. E.; DeSimone, J. M., The effect of particle design on cellular internalization pathways. *Proceedings of the National Academy of Sciences, USA* **2008,** *105* (33), 11613-11618.
16. Lipowsky, R.; Seifert, U., Adhesion of vesicles and membranes. *Molecular Crystals and Liquid Crystals* **1991,** *202* (1), 17-25.
17. Seifert, U.; Lipowsky, R., Adhesion of vesicles. *Physical Review A* **1990,** *42* (8), 4768.
18. Oh, E.; Jackman, J. A.; Yorulmaz, S.; Zhdanov, V. P.; Lee, H.; Cho, N.-J., Contribution of Temperature to Deformation of Adsorbed Vesicles Studied by Nanoplasmonic Biosensing. *Langmuir* **2015,** *31* (2), 771-781.
19. Hain, N.; Gallego, M.; Reviakine, I., Unraveling supported lipid bilayer formation kinetics: osmotic effects. *Langmuir* **2013,** *29* (7), 2282-2288.
20. Jackman, J. A.; Choi, J.-H.; Zhdanov, V. P.; Cho, N.-J., Influence of osmotic pressure on adhesion of lipid vesicles to solid supports. *Langmuir* **2013,** *29* (36), 11375-11384.
21. Pencer, J.; White, G. F.; Hallett, F. R., Osmotically induced shape changes of large unilamellar vesicles measured by dynamic light scattering. *Biophysical journal* **2001,** *81* (5), 2716-2728.
22. Saveyn, P.; Cocquyt, J.; Bomans, P.; Frederik, P.; De Cuyper, M.; Van der Meeren, P.,

Osmotically induced morphological changes of extruded dioctadecyldimethylammonium chloride (DODAC) dispersions. *Langmuir* **2007,** *23* (9), 4775-4781.
23. Jackman, J. A.; Špačková, B.; Linardy, E.; Kim, M. C.; Yoon, B. K.; Homola, J.; Cho, N.-J., Nanoplasmonic ruler to measure lipid vesicle deformation. *Chemical Communications* **2016,** *52* (1), 76-79.
24. Dacic, M.; Jackman, J. A.; Yorulmaz, S.; Zhdanov, V. P.; Kasemo, B.; Cho, N.-J., Influence of Divalent Cations on Deformation and Rupture of Adsorbed Lipid Vesicles. *Langmuir* **2016,** *32* (25), 6486-6495.
25. Tabaei, S. R.; Gillissen, J. J.; Kim, M. C.; Ho, J. C.; Parikh, A. N.; Cho, N.-J., Brownian Dynamics of Electrostatically Adhering Nano-Vesicles on a Membrane Surface Induces Domains and Probes Viscosity. *Langmuir* **2016**.
26. Tabaei, S. R.; Gillissen, J. J. J.; Cho, N. J., Probing Membrane Viscosity and Interleaflet Friction of Supported Lipid Bilayers by Tracking Electrostatically Adsorbed, Nano-Sized Vesicles. *Small* **2016,** *12* (46), 6338-6344.
27. Tabaei, S. R.; Gillissen, J. J.; Block, S.; Hook, F.; Cho, N. J., Hydrodynamic Propulsion of Liposomes Electrostatically Attracted to a Lipid Membrane Reveals Size-Dependent Conformational Changes. *ACS Nano* **2016,** *10* (9), 8812-20.
28. Lee, G. M.; Ishihara, A.; Jacobson, K. A., Direct observation of Brownian motion of lipids in a membrane. *Proceedings of the National Academy of Sciences* **1991,** *88* (14), 6274-6278.
29. Yoshina-Ishii, C.; Chan, Y.-H. M.; Johnson, J. M.; Kung, L. A.; Lenz, P.; Boxer, S. G., Diffusive dynamics of vesicles tethered to a fluid supported bilayer by single-particle tracking. *Langmuir* **2006,** *22* (13), 5682-5689.
30. Hormel, T. T.; Kurihara, S. Q.; Brennan, M. K.; Wozniak, M. C.; Parthasarathy, R., Measuring lipid membrane viscosity using rotational and translational probe diffusion. *Physical review letters* **2014,** *112* (18), 188101.
31. Evans, E.; Sackmann, E., Translational and rotational drag coefficients for a disk moving in a liquid membrane associated with a rigid substrate. *Journal of Fluid Mechanics* **1988,** *194*, 553-561.
32. Subramaniam, S.; Seul, M.; McConnell, H., Lateral diffusion of specific antibodies bound to lipid monolayers on alkylated substrates. *Proceedings of the National Academy of Sciences* **1986,** *83* (5), 1169-1173.
33. Kunze, A.; Svedhem, S.; Kasemo, B., Lipid transfer between charged supported lipid bilayers and oppositely charged vesicles. *Langmuir* **2009,** *25* (9), 5146-5158.
34. Israelachvili, J. N., *Intermolecular and surface forces: revised third edition*. Academic press: 2011.
35. Asakura, S.; Oosawa, F., On interaction between two bodies immersed in a solution of macromolecules. *The Journal of Chemical Physics* **1954,** *22* (7), 1255-1256.
36. Trokhymchuk, A.; Henderson, D., Depletion forces in bulk and in confined domains: From Asakura–Oosawa to recent statistical physics advances. *Current Opinion in Colloid & Interface Science* **2015,** *20* (1), 32-38.
37. Papahadjopoulos, D., Na+-K+ discrimination by "pure" phospholipid membranes. *Biochimica et Biophysica Acta (BBA)-Biomembranes* **1971,** *241* (1), 254-259.
38. Takechi-Haraya, Y.; Sakai-Kato, K.; Abe, Y.; Kawanishi, T.; Okuda, H.; Goda, Y., Atomic Force Microscopic Analysis of the Effect of Lipid Composition on Liposome Membrane Rigidity. *Langmuir* **2016**.
39. Gillissen, J. J.; Jackman, J. A.; Tabaei, S. R.; Cho, N.-J., A Quartz Crystal Microbalance Model for Quantitatively Probing the Deformation of Adsorbed Particles at Low Surface Coverage. *Analytical Chemistry* **2017**.
40. Saffman, P.; Delbrück, M., Brownian motion in biological membranes. *Proceedings of the National Academy of Sciences* **1975,** *72* (8), 3111-3113.

41. Kalb, E.; Frey, S.; Tamm, L. K., Formation of supported planar bilayers by fusion of vesicles to supported phospholipid monolayers. *Biochimica et Biophysica Acta (BBA) - Bioenergetics* **1992,** *1103* (2), 307-16.
42. Jönsson, P.; Beech, J. P.; Tegenfeldt, J. O.; Höök, F., Mechanical behavior of a supported lipid bilayer under external shear forces. *Langmuir* **2009,** *25* (11), 6279-6286.
43. Evans, E.; Yeung, A., Hidden dynamics in rapid changes of bilayer shape. *Chemistry and Physics of Lipids* **1994,** *73* (1), 39-56.
44. Merkel, R.; Sackmann, E.; Evans, E., Molecular friction and epitactic coupling between monolayers in supported bilayers. *Journal de Physique* **1989,** *50* (12), 1535-1555.
45. Cicuta, P.; Keller, S. L.; Veatch, S. L., Diffusion of liquid domains in lipid bilayer membranes. *The journal of physical chemistry B* **2007,** *111* (13), 3328-3331.
46. Angelova, M.; Soleau, S.; Méléard, P.; Faucon, F.; Bothorel, P., Preparation of giant vesicles by external AC electric fields. Kinetics and applications. In *Trends in colloid and interface science VI*, Springer: 1992; pp 127-131.
47. Helfrich, W., Effect of thermal undulations on the rigidity of fluid membranes and interfaces. *Journal de Physique* **1985,** *46* (7), 1263-1268.
48. Przybylo, M.; Sýkora, J.; Humpolíčková, J.; Benda, A.; Zan, A.; Hof, M., Lipid diffusion in giant unilamellar vesicles is more than 2 times faster than in supported phospholipid bilayers under identical conditions. *Langmuir* **2006,** *22* (22), 9096-9099.
49. Saffman, P., Brownian motion in thin sheets of viscous fluid. *Journal of Fluid Mechanics* **1976,** *73* (4), 593-602.
50. Dimova, R., Recent developments in the field of bending rigidity measurements on membranes. *Advances in colloid and interface science* **2014,** *208*, 225-234.
51. Gillissen, J. J. J.; Tabaei, S. R.; Jackman, J. A.; Cho, N. J., A model derived from hydrodynamic simulations for extracting the size of spherical particles from the quartz crystal microbalance. *Analyst* **2017,** *142* (18), 3370-3379.
52. Kuhl, T.; Guo, Y.; Alderfer, J. L.; Berman, A. D.; Leckband, D.; Israelachvili, J.; Hui, S. W., Direct measurement of polyethylene glycol induced depletion attraction between lipid bilayers. *Langmuir* **1996,** *12* (12), 3003-3014.
53. Ariga, K.; Minami, K.; Ebara, M.; Nakanishi, J., What are the emerging concepts and challenges in NANO? Nanoarchitectonics, hand-operating nanotechnology and mechanobiology. *Polymer Journal* **2016,** *48* (4), 371-389.
54. Lei, G.; MacDonald, R. C., Lipid bilayer vesicle fusion: intermediates captured by high-speed microfluorescence spectroscopy. *Biophysical journal* **2003,** *85* (3), 1585-1599.
55. Solon, J.; Pécréaux, J.; Girard, P.; Fauré, M.-C.; Prost, J.; Bassereau, P., Negative tension induced by lipid uptake. *Physical review letters* **2006,** *97* (9), 098103.